

Minimum Efforts to Build an End-to-End Spatial-Temporal Action Detector

Lin Sui^{1,2}, Chen-Lin Zhang^{1*}, Lixin Gu¹, and Feng Han¹

¹ 4Paradigm Inc., Beijing, China

² State Key Laboratory for Novel Software Technology, Nanjing University, China
{suilin0432, zclnjucs}@gmail.com {gulixin, hanfeng}@4paradigm.com

Abstract Spatial-temporal action detection is a vital part of video understanding. Current spatial-temporal action detection methods will first use an object detector to obtain person candidate proposals. Then, the model will classify the person candidates into different action categories. So-called two-stage methods are heavy and hard to apply in real-world applications. Some existing methods use a unified model structure, But they perform badly with the vanilla model and often need extra modules to boost the performance. In this paper, we explore the strategy to build an end-to-end spatial-temporal action detector with minimal modifications. To this end, we propose a new method named ME-STAD, which solves the spatial-temporal action detection problem in an end-to-end manner. Besides the model design, we propose a novel labeling strategy to deal with sparse annotations in spatial-temporal datasets. The proposed ME-STAD achieves better results (2.2% mAP boost) than original two-stage detectors and around 80% FLOPs reduction. Moreover, our proposed ME-STAD only has minimum modifications with previous methods and does not require extra components. Our code will be made public.

Keywords: Spatial-Temporal Action Detection, End-to-End Action Detection

1 Introduction

Spatial-temporal action detection (STAD), which aims to classify the person’s actions in videos, is a vital part of video understanding. The computer vision community has drawn much attention in the field of STAD [35,7,41].

In previous methods, STAD is often divided into two sub-tasks: actor localization and action classification. Previous methods mostly utilize a pre-trained object detector [32,44] and finetune it on the target dataset to obtain person candidates. Then, proposals are fed into the action classifier network to obtain the final action prediction. However, those two-stage methods are heavy and often need extra data (such as MS-COCO [23]). They need separate models and heavy

* Corresponding author

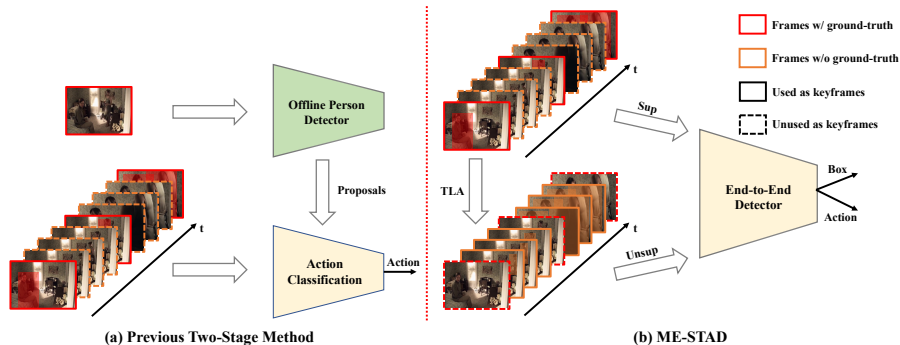


Figure 1. Comparison between previous two-stage methods and our ME-STAD. (a). Previous two-stage STAD methods use a heavy offline person detector, which also rely on additional data, to perform actor localization and they only use annotations of keyframes to train the action classifier. (b). Our ME-STAD trains an end-to-end spatial-temporal action detector in which actor localization part only occupies a small part of the computation. We also propose temporal label assignment (TLA) to utilize unlabeled frames in large-scale sparsely annotated datasets like AVA [13].

computational resources. This prevents the current methods from real-world applications. A recent work [5] has shown that there is a dilemma between actor localization and action classification. Actor localization only needs a single image while action detection needs the whole input sequence. Thus, [5] proposes an end-to-end method WOO, which uses a unified backbone to perform actor localization and action detection. However, they still have a significant performance drop with the vanilla structure and need to introduce an additional attention module into the action classification head to enhance the performance.

In this paper, we first investigate the current drawbacks of existing two-stage and single-stage methods. Based on the investigation, we propose a new method named **Minimum Efforts Spatial-Temporal Action Detection**, in short for ME-STAD. The general pipeline of ME-STAD is in Fig. 1. ME-STAD proposes minimum modifications to the current framework. With minor added components, we empower the ability to conduct actor localization and action classification simultaneously. Compared to existing works, our work is light-weighted and joint optimized, which avoids the separate learning problem. Besides, our work avoids extra attention modules like previous works to keep a clean baseline.

Besides the model design, we also develop a new paradigm to utilize every possible information in sparsely annotated spatial-temporal datasets. Sparse annotation is an efficient and effective way to build a large-scale STAD dataset, only the keyframes will be annotated (e.g. 1fps in AVA [13]). A huge amount of frames do not have annotations. Hence, we propose to utilize these unlabeled data to provide more clear temporal action boundaries and help the detector to learn fine-grained information. Considering the distinctiveness of unlabeled data in sparse-annotated STAD datasets, we propose a novelty pseudo labeling

strategy: temporal label assignment (TLA) to generate pseudo labels. With the help of TLA, spatial-temporal action detectors successfully enjoy performance gains from the neglected unlabeled data of sparse-annotated datasets.

Our contributions are listed as follows:

- We propose a minimum modification to the current proposal-based spatial-temporal action detection framework and build an end-to-end spatial-temporal action detector with comparable performance to proposal-based methods.
- We propose a novel semi-supervised learning strategy with a pseudo temporal labeling strategy to utilize every possible information in sparsely annotated data and boost the performance in spatial-temporal action detection.
- With the proposed model and learning strategy, we achieve a 2.2% mAP boost and around 80% FLOPs reduction compared to the commonly used SlowFast R50 with extra proposals, and we achieve a 1.5% mAP boost and around 20% FLOPs reduction with the recent unified spatial-temporal action detection methods.

2 Related Works

In this section, we will introduce works related to our ME-STAD, including spatial-temporal action detection, object detection and semi-supervised learning.

2.1 Spatial-Temporal Action Detection

Spatial-temporal action detection (STAD) aims to detect the spatial and temporal location of the person in the input video clips. Thus, the spatial-temporal action detection model needs to be aware of spatial and temporal information. After the large-scale datasets are annotated and introduced [13,18], researchers have paid much attention to spatial-temporal action detection.

Early works often follow a traditional Fast-RCNN [10] pipeline with pre-extracted proposals to perform STAD [13,19,41,28]. A previous work [42] shows the original R-CNN [11] pipeline works better for spatial-temporal action detection. However, those works are heavy and not effective.

Besides those two-stage methods, researchers also proposed some single-stage methods for action detection. Some works [13,8] also employ the Faster-RCNN [32] pipeline but with low efficiency. Early works including YOWO [15], ACRN [35] and Point3D [27] propose to use 2D CNN backbone for actor localization and 3D CNN backbone for action detection to build end-to-end spatial-temporal action detectors. However, those models use two separate models to conduct two tasks independently and also need the weights from 2D and 3D backbones pretrained on large-scale image and video datasets. Recently, WOO [5] proposes a single-stage, unified network for end-to-end action detection. However, WOO utilizes an extra attention module to boost performance. With the vanilla structure, WOO has a major performance gap with the proposal-based methods. In contrast, our proposed ME-STAD has a minimum modification to

the current proposal-based method, and we achieve much better results than WOO and better than proposal-based methods with an extra person detector.

Apart from the detection structure side, Many researchers also propose new modules to enhance the performance. Feature bank methods are often applied in STAD to capture long-term dependencies [41,28]. Attention modules are often applied to enhance performance [28,5]. Graph-based modules are also popular in recent spatial-temporal action detection methods [9,35,47]. However, we want to build a clean and simple model for end-to-end spatial-temporal action detection. Thus, we do not add any extra modules to our ME-STAD.

2.2 Object Detection

Actor localization needs to detect the spatial location of persons in the input image. Thus, object detection is needed for actor localization. Object detection has been a popular area in the computer vision community. Early works often use a two-stage pipeline with pre-defined anchors [11,10,32]. One-stage methods are proposed to reduce the computational burden for object detection [22,31,24]. In one-stage detectors, anchor-free (i.e., point-based) detectors has attracted much attention in recent computer vision community [38,48]. Anchor-free detectors are easy to use in real-world applications. More recent methods want to train object detectors in an end-to-end manner [3,36] without postprocessing steps.

In this paper, we adopt the popular one-stage anchor-free method FCOS [38], as the person detector in our ME-STAD. FCOS is a simple, effective and efficient baseline for the person detector.

2.3 Semi-Supervised Learning

Semi-supervised learning (SSL) aims to achieve better performance with the help of additional unlabeled data. In brief, recent semi-supervised learning follows two main ways: introducing consistency regularization [30,2,43] or performing pseudo-labeling [17,37,39]. Some other works, such as [34] also combine these two ways into a single method. Consistency regularization often emphasizes the prediction consistency among different views of the same image to build robust models. Pseudo-labeling stresses on generating high-quality pseudo labels for unlabeled data to further update the network.

Semi-supervised object detection (SSOD), which has received lots of attention recently, is an important sub domain in SSL, and there exist some overlaps between object detection and spatial-temporal action detection. CSD [14] used the consistency of predictions and proposed background elimination. Some other works [25,46,45] built variants of the Mean Teacher [37] framework and achieved promising performance gains.

However, in traditional semi-supervised learning tasks such as SSOD and semi-supervised classification, the unlabeled data is introduced additionally without any temporal restrictions. Whereas, in large-scale sparsely annotated STAD datasets such as AVA [13], the unlabeled frames have high correlation with the

nearby labeled frames. Temporal restriction between the labeled part and the unlabeled part has not been explored in the STAD field yet.

3 Methods

In this section, we will give a detailed description of our ME-STAD.

3.1 Notations

We will first define the notations used in this paper.

Given a spatial-temporal action detection dataset \mathcal{D} , which is composed of a total number of m videos: $\mathcal{D} = \{V_1, \dots, V_m\}$. For simplicity, we suppose all videos in \mathcal{D} have same height h , width w and number of frames n . Thus, $V_i \in \mathbb{R}^{n \times h \times w \times 3}$. Spatial temporal action detection needs to detect the action category of the person in the specific input frame. For a frame F_j in V_i , we need to detect a tuple (x_1, y_1, x_2, y_2, c) for each person in F_j . (x_1, y_1, x_2, y_2) is the spatial location of the person, and $c \in [0, 1]^C$ is the action category where C is the pre-defined set of action classes. In widely used sparse-annotated datasets such as AVA [13], ground-truth annotations are annotated at one frame per second. For such a dataset \mathcal{D} , We denotes the labeled part as $\mathcal{D}^l = \{V_1^l, \dots, V_m^l\}$ with annotations $Y^l = \{A_1^l, \dots, A_m^l\}$ and the unlabeled part as $\mathcal{D}^u = \{V_1^u, \dots, V_m^u\}$.

3.2 Motivation

As shown in Sec. 2, previous STAD methods often follow a two-stage pipeline and utilize two networks: First conducting person detection with an offline object detector, then detected area of interests (RoIs) will be fed into a traditional Fast-RCNN style network to obtain the final action predictions. The two-stage networks are not efficient. Besides, they always need extra data (such as MS-COCO [23]) to train the additional person detector. WOO [5] uses a unified backbone to perform actor localization and action classification simultaneously. However, their unified models result in a large performance drop and WOO [5] proposes an extra embedding interaction head to boost the performance.

In contrast to those extra modules, we want to build a unified, end-to-end and simple method for spatial-temporal action detection. Thus, we want to make minimal modifications to current proposal-based methods, to perform spatial-temporal action detection effectively and efficiently. We name our proposed model as **Minimal Efforts Spatial Temporal Action Detection (ME-STAD)**.

3.3 ME-STAD

Our proposed ME-STAD is composed of three parts: feature extraction part, actor localization part and action classification part. We unified the three parts into a single network. We will introduce these three parts step by step.

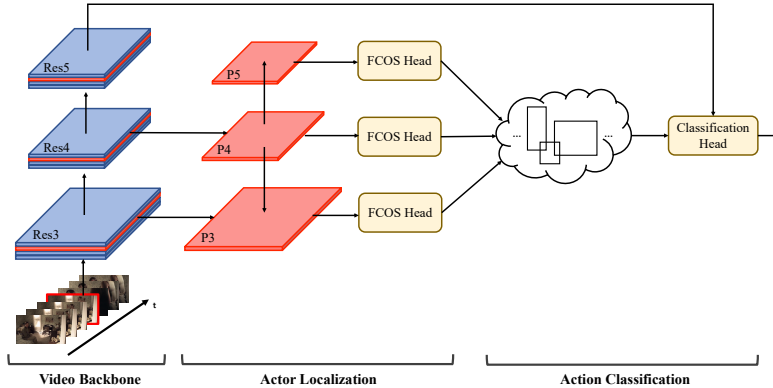


Figure 2. Overview of our ME-STAD. The whole pipeline consists of three parts: video backbone, actor localization part and action classification part. In the actor localization part, we build the feature pyramid on top of keyframes feature from Res3 and Res4 layers. After performing actor localization, proposals generated by FCOS heads will be used to extract features from Res5 and perform action classification.

Feature Extraction In this part, we directly use existing action classification backbones, i.e., SlowFast [7] for feature extraction. Moreover, our proposed ME-STAD can utilize any modern backbones to boost the performance, including the recent Transformer-based models, i.e., Video-Swin [26], ViViT [1] and MViT [6].

Actor Localization Part We need to perform actor localization in our ME-STAD. Previously, separate pre-trained object detectors are adopted on actor localization, the most commonly used are Faster-RCNN [32] with a ResNeXt [44] backbone. However, the separate object detector has an extra heavy computational burden, which is inefficient. A recent work WOO [5] proposes to integrate an existing object detection head, i.e., Sparse R-CNN [36] into the current action classification backbone. In this paper, we follow the suggestions in WOO [5], performing actor localization with the spatial feature of keyframes. Regarding the low input resolution and efficiency issue, we choose a popular one-stage anchor-free object detector FCOS [38]. Thus, the loss for actor localization is:

$$\mathcal{L}_{al} = \mathcal{L}_{cls}(\mathbf{c}_i, \mathbf{b}_i) + \mathcal{L}_{iou}(\mathbf{c}_i, \mathbf{b}_i) + \mathcal{L}_{centerness}(\mathbf{c}_i, \mathbf{b}_i) \quad (1)$$

where \mathbf{c}_i indicates the video clip, \mathbf{b}_i means ground-truth bounding boxes of the keyframe of \mathbf{c}_i . \mathcal{L}_{cls} , \mathcal{L}_{iou} and $\mathcal{L}_{centerness}$ are the Focal loss [22] for binary classification (existing of actor), GIoU [33] loss for bounding box regression and centerness prediction, respectively. In Sec. 4, We ablate different heads for actor localization including anchor-based heads and anchor-free heads to verify the effectiveness of different heads. Our models use a simple actor localization head and perform better than vanilla WOO [5], even comparable or better than WOO with extra attention modules. We provide detailed analyses in Sec. 4.

Action Classification Part For action classification, since we want to build an end-to-end spatial-temporal action detection network with minimum efforts, we follow the common practice to build an action classification head: we use the traditional ROIAlign [22] layer with temporal pooling to get the feature for each actor proposal, then a simple linear layer is attached to get the final action predictions, we use the binary cross entropy loss to train the action classification head. Thus, the loss of the action classification head becomes:

$$\mathcal{L}_{ac} = \mathcal{L}_{bce}(\mathbf{c}_i, \mathbf{b}_i, \mathbf{l}_i) \quad (2)$$

where \mathbf{l}_i denotes the classification annotation and \mathcal{L}_{bce} is binary cross entropy loss. In order to balance the scale of localization loss \mathcal{L}_{al} and classification loss \mathcal{L}_{ac} , we introduce loss weight λ_{cls} for action classification which is set to 10 as default. Experiments in Sec. 4 show the model is robust to different λ_{cls} .

The overall structure of our ME-STAD is quite simple. We only add a simple FCOS head to perform actor localization. However, a simple model achieves comparable results to proposal-based methods [7] and the recently unified backbone method [5] which introduces additional attention modules.

Besides the model structure, we propose a novel semi-supervised training strategy to better utilize every possible piece of information in the training video. With the semi-supervised training stage, our model can achieve better results than originally trained models.

3.4 Semi-Supervised Action Detection for ME-STAD

It’s well known that sparse annotation is an efficient and effective way to build large-scale spatial-temporal action detection datasets. However, as large parts of data are unlabeled, sparse annotations fail to provide clear temporal action boundaries. This phenomenon has been shown by previous literature [21]. Utilizing the unlabeled part is a natural way to help the detector to learn fine-grained information. Hence, we propose a new semi-supervised training method for sparsely annotated datasets in spatial-temporal action detection.

When performing semi-supervised training in ME-STAD, we adopt the online updating paradigm. Besides, in order to avoid the inductive bias introduced in semi-supervised training, following the widely used Mean Teacher [37] pipeline, we also build a teacher-student mutual-learning paradigm. Firstly, to get a good initialization for the detector, we do not perform semi-supervised training directly at first. That means we only use data with annotations to warm up the detector D by Eq. 3.

$$\mathcal{L}_{sup} = \frac{1}{N} \sum_i \mathcal{L}_{ac}(\mathbf{c}_i^s, \mathbf{b}_i^s, \mathbf{l}_i^s) + \lambda_{cls} \mathcal{L}_{al}(\mathbf{c}_i^s, \mathbf{b}_i^s) \quad (3)$$

After warming up the spatial-temporal action detector D , weights of D will be copied to the teacher model $D_{teacher}$ and student model $D_{student}$ as the initialization weights. Then we use both the labeled data and unlabeled data

Algorithm 1 Temporal Label Assignment (TLA)

Input: video clip \mathbf{c}^u , boxes and labels of nearest former keyframe $\mathbf{b}^{left}, \mathbf{l}^{left}$ and nearest later keyframe $\mathbf{b}^{right}, \mathbf{l}^{right}$, detector D

Output: pseudo bounding boxes \mathbf{b}^u , pseudo labels \mathbf{l}^u

- 1: $\mathbf{b}^u, \mathbf{s} = D(\mathbf{c}^u)$
- 2: $\mathbf{b}^{gt} = \mathbf{b}^{left} \cup \mathbf{b}^{right}, \mathbf{l}^{gt} = \mathbf{l}^{left} \cup \mathbf{l}^{right}$
- 3: **for** $i = 1, \dots, N$
- 4: **for** $j = 1, \dots, M$
- 5: $Cost_{ij} = \mathcal{L}_{bce}(\mathbf{s}_i, \mathbf{l}_j^{gt}) + \mathcal{L}_{L1}(\mathbf{b}_i^u, \mathbf{b}_j^{gt}) + \mathcal{L}_{iou}(\mathbf{b}_i^u, \mathbf{b}_j^{gt})$
- 6: Label assignment policy $\hat{\pi} = \arg \min_{\pi \in \Pi_N^M} \sum_i^N Cost_{i, \pi(i)}$
- 7: $inds = [\hat{\pi}(1), \dots, \hat{\pi}(N)]$
- 8: $\mathbf{l}^u = \mathbf{l}_{gt}[inds]$

to further train the detector. The student model is updated via gradient back-propagation, but the gradient back-propagating to the teacher model is stopped. The teacher model is maintained by exponential moving average so as to eliminate the influence of inductive bias and provide more accurate person proposals for the student at the beginning. Loss function in this stage consists of losses on labeled data \mathcal{L}_{sup} (Eq. 3) and unlabeled data \mathcal{L}_{unsup} (Eq. 5).

$$\mathcal{L} = \mathcal{L}_{sup} + \lambda_{unsup} \mathcal{L}_{unsup} \quad (4)$$

$$\mathcal{L}_{unsup} = \frac{1}{N} \sum_i \mathcal{L}_{ac}(\mathbf{c}_i^u, \mathbf{b}_i^u, \mathbf{l}_i^u) + \lambda_{cls} \mathcal{L}_{al}(\mathbf{c}_i^u, \mathbf{b}_i^u) \quad (5)$$

where \mathbf{b}_i^u and \mathbf{l}_i^u are pseudo ground-truth annotations dynamically generated by temporal label assignment (TLA) which will be discussed later.

As the spatial-temporal action detection tasks are always accompanied by multi-label and long-tail classification problems, pseudo-labels have a high risk ratio of missing tags and inaccuracies, especially for the rare categories with poor classification performance. Besides, we found that the temporal constraints are strong in spatio-temporal data. Therefore, we propose temporal label assignment (TLA) to assign classification labels for unlabeled data. Because the temporal actions are highly bounded by the temporal restrictions, we propose TLA to assign pseudo labels to detected person proposals by utilizing the neighbour annotated keyframes. The TLA procedure is detailed in Algorithm 1. Firstly, $D_{teacher}$ generates person proposals \mathbf{b}^u and classification scores \mathbf{s} for a video clip $\mathbf{c}^u \in \mathcal{D}^u$ with unlabeled center frame. We fetch the ground-truth bounding boxes $\mathbf{b}^{left}, \mathbf{b}^{right}$ and classification labels $\mathbf{l}^{left}, \mathbf{l}^{right}$ of the neighbour annotated keyframes which are nearest to center frame of \mathbf{c}^u to perform TLA. Then we assign pseudo-labels to person proposals by resorting to the help of Hungarian algorithm. Following [3], we consider both classification and regression factors and build the cost function between i -th prediction and j -th annotation as Eq. 6.

$$Cost_{ij} = \mathcal{L}_{bce}(\mathbf{s}_i, \mathbf{l}_j^{gt}) + \mathcal{L}_{L1}(\mathbf{b}_i^u, \mathbf{b}_j^{gt}) + \mathcal{L}_{iou}(\mathbf{b}_i^u, \mathbf{b}_j^{gt}) \quad (6)$$

where \mathcal{L}_{bce} , \mathcal{L}_{L1} and \mathcal{L}_{iou} are binary cross entropy loss, smooth-L1 loss and GIoU loss. Weights of loss functions are set to 1. Then we use Hungarian algorithm [16] to calculate the optimal label assignment policy $\hat{\pi}$ to minimize Eq. 7.

$$\hat{\pi} = \arg \min_{\pi \in \Pi_N^M} \sum_i^N Cost_{i, \pi(i)} \quad (7)$$

Finally, we can use $\hat{\pi}$ to assign pseudo classification label $\mathbf{1}_{\hat{\pi}(i)}^{gt}$ to i -th person boxes \mathbf{b}_i^u . Each ground-truth bounding boxes could only be assigned to one person proposal. If the number of proposals N is larger than the number ground-truth bounding boxes M , additional background objects will be added. The cost between one prediction and one background object only contains the classification part (i.e. the binary cross entropy loss).

4 Experiments

In this section, we will provide the experiments settings, results, and ablations.

4.1 Experimental Setup

Datasets AVA [13] is a major dataset for benchmarking the performance for spatial-temporal action detection. It contains about 211k training clips and 57k validating video clips. The labels are annotated at 1FPS, i.e., one frame is annotated per second. every person is annotated with a bounding box and action labels. Following standard evaluation protocol [13,8,7], we evaluate 60 classes among total 80 classes. AVA has two versions of annotations: AVA v2.1 and AVA v2.2, we evaluate on both versions of annotations.

Training Details We use a server with 3090 GPUs to conduct all our experiments. We use PyTorch [29] to implement our ME-STAD. To conduct a fair comparison, we adopt the commonly used backbone, SlowOnly and SlowFast [7] network as our backbone. We use SlowOnly ResNet50, SlowFast ResNet50 and SlowFast ResNet101 with non-local [40] modules to perform experiments. For actor localization head, we use an improved version of FCOS [38], i.e., FCOS with center sampling as our actor localization head.

Following previous works [8,7], we use SGD with momentum as our optimizer. The hyperparameters are listed as follows: The batch size is 48 with 8 GPUs (6 clips per GPU) for the burn-in (baseline) stage, and 96 in the semi-supervised action detection (SSAD) stage. the ratio of labeled/unlabeled data is 1:1 in the SSAD stage. We use an initial learning rate of 0.075 and the cosine decay schedule. We train the model with 20000 iterations (around 5 epochs) in the burn-in stage, and we train the model with 40000 iterations (around 10 epochs) in the SSAD stage. For models without SSAD, we train the model with 40000 iterations. Longer training schedule (60000 or 80000 iterations) will decrease the

performance by around 0.3% mAP when adopting SlowFast R50 backbone. The backbone is initialized with the pre-trained weights on Kinetics-400 or Kinetics-600 [4]. The actor localization head uses the initialization schedule in the original FCOS [38] paper. For other layers, we initialize the layer with Xavier [12]. We perform random scaling to the video clip input, we random resize the shortest edge to [256, 320]. and then we random crop a 256×256 video clip to feed into the model.

For the actor localization head, we will use a post-processing step with 0.3 scoring threshold and maximum number of 100 proposals during training. We do not perform non-maximum suppression (NMS) for actor localization head in the training stage. Then those proposals will be fed into the action classification head. The loss is showed in Sec. 3. The loss weight for \mathcal{L}_{al} is 1 and 10 for \mathcal{L}_{ac} . Generated proposals which have at least 50% intersection-over-union (IoU) with the ground-truth boxes will be treated as positive proposals in the action classification stage, otherwise those proposals will be ignored.

Testing Details Our inference steps are somehow simple. With an input video clip, we will first resize the shortest edge to 256, then directly feed into the model. We will use a post-processing step with 0.4 scoring threshold and NMS step with IoU threshold 0.3 to get the testing proposals. Then those proposals will be fed into the action classification head. We set the final action threshold as 0.002 and limit the maximum output of actors to 10 per image. During inference, we always use a single view instead of applying multi-scale testing to our models.

4.2 Results on AVA

In this section, we will provide results and analyses of results on AVA. The results are listed in Table 1. From the table, we can have following observations:

- Extra person detector will bring a huge computational burden to the spatial-temporal action detection model. The FLOPs of the person detector is 406.5G FLOPs. which is around 7 times larger than the FLOPs of SlowOnly R50 (4×16), and more than 2 times larger than the heaviest backbone SlowFast R101-NL (8×8). The large FLOPs come from the high input resolution in the person detector. The high input resolution along with the high FLOPs makes proposal-based methods hard to apply in real-world scenarios.
- With a simply added component, i.e., FCOS head, our model can have roughly comparable or better performance than proposal-based methods, even than the recent WOO [5] and we do not use extra SSAD techniques. This is quite encouraging because we have an around 70~90% FLOPs drop with proposal-based SlowFast, and we have around 20~35% FLOPs drop with WOO [5]. This shows the effectiveness of our simple models. We will dive into the model details part to figure out what makes the simple model work so well.
- With the extra SSAD techniques (the semi-supervised learning stage and the temporal labeling assignment), our model can have an extra performance

Table 1. Results on AVA dataset. We report the FLOPs of action classification network plus the FLOPs of person detector for proposal-based methods. We calculate the FLOPs of person detector according to the official configure file provided by [41]. * means the method reports the performance by testing with 320 resolution.

AVA	Model	Backbone	Frames	E2E	Pretrain	val mAP	GFLOPs
AVA v2.1	VAT [9]	I3D	64	✗	K400	25.2	N/A
	I3D [8]	I3D	64	✓	K400	21.9	N/A
	Context-RCNN [42]	R50-NL	64	✗	K400	28.0	N/A
	LFB [41]	R50-NL	64	✗	K400	25.8	N/A
	LFB [41]	R101-NL	64	✗	K400	27.1	N/A
	SlowFast [7]		32	✗	K400	24.7	97.5+406.5
	WOO* [5]	R50	32	✗	K400	25.2	141.6
	ME-STAD	8 × 8	32	✓	K400	25.0	111.3
	ME-STAD + TLA		32	✓	K400	26.5	111.3
	SlowFast [7]		32	✗	K600	27.3	151.5+406.5
	WOO* [5]	R101-NL	32	✓	K600	28.0	245.8
	ME-STAD	8 × 8	32	✓	K600	27.7	165.2
	ME-STAD + TLA		32	✓	K600	28.8	165.2
	AVA v2.2	SlowOnly [7]		4	✗	K400	20.3
WOO* [5]		R50	4	✓	K400	21.3	68.0
ME-STAD		4 × 16	4	✓	K400	21.5	55.5
ME-STAD + TLA			4	✓	K400	22.0	55.5
SlowFast [7]			32	✗	K400	24.7	97.5+406.5
WOO* [5]		R50	32	✓	K400	25.4	147.5
ME-STAD		8 × 8	32	✓	K400	25.5	111.3
ME-STAD + TLA			32	✓	K400	26.9	111.3
SlowFast [7]			32	✗	K600	27.4	151.5+406.5
WOO* [5]		R101-NL	32	✓	K600	28.3	251.7
ME-STAD		8 × 8	32	✓	K600	28.5	165.2
ME-STAD + TLA			32	✓	K600	29.3	165.2

boost with no extra modules and no computational cost. For example, SlowFast R50 can have an extra 1.4% mAP performance boost on AVA v2.2 and 1.5% mAP boost on AVA v2.1. Similar performance gap are observed on SlowFast R101. However, SSAD stage can only have a 0.5% performance gain on SlowOnly R50. We conjecture that it may due to the input capacity. SlowOnly R50 only has 4 frames as input. The low number of input frames prevents SlowOnly R50 to have better performance gain with SSAD techniques.

4.3 Ablation Study

In this section, we will provide ablations of our model, including the head choice for actor localization, loss coefficients, input resolutions and the methods to train the action classification. In this section, unless specified, all experiments use SlowFast R50 (8 × 8) as the backbone network.

Actor Heads	Type	<i>mAP</i>
RPN+RCNN [32]	Anchor-Based	21.0
RetinaNet [22]	Anchor-Based	19.7
GFocalV2 [20]	Anchor-Based	23.7
FCOS- [38]	Anchor-Free	24.9
WOO* [5]	Anchor-Free	25.4
FCOS [38]	Anchor-Free	25.5

Table 2. Ablation study on different heads for actor localization.

We try different heads (anchor-free heads and anchor-based heads) with SlowFast R50 backbone. We apply the anchor-based version of GFocalV2 [20] in this table. FCOS- is the original FCOS [38] version without tricks. We do not use self/semi-training for all our methods. WOO [5] is listed here only for comparison.

Training input	Testing input	<i>mAP</i>
Proposal	Proposal	24.7
GT Only	Proposal	24.5
GT Only	FCOS Output	23.7
FCOS Output (Sparse)	FCOS Output	24.3
FCOS Output (Dense)	FCOS Output	25.5
FCOS Output (Dense)	Proposal	26.2

Table 3. Ablation study on different training inputs for action classification.

We try different inputs for both training and testing of our models. For “GT Only”, we only feed the ground-truth boxes into the action classification head. For “FCOS Output (Sparse)”, we perform NMS to FCOS generated proposals in the training stage. For “FCOS Output (Dense)”, we do not perform NMS in the training stage.

Head Choices for Actor Localization In this section, we vary the head of actor localization for ME-STAD. We try different heads, including the popular anchor-based heads: RPN + RCNN [32], RetinaNet [22] and GFocalV2 [20]. The ablation results are in Table 2. From Table 2 we can observe that, Anchor-based heads perform significantly worse than anchor-free heads, i.e., FCOS [38]. Two-stage RPN+RCNN [32] and RetinaNet [22] have a large performance drop. Even the most recent GFocalV2 head (anchor-based version) will have a 1.8% *mAP* gap with the FCOS head. Besides, tricks on FCOS will improve around 0.6% *mAP*, and the original FCOS head will still achieve a 24.9% *mAP*. It may due to the low input resolution and pre-defined anchor shape. Moreover, with the simple FCOS head, our model performs slightly better than WOO [5]. WOO has an extra attention module. In contrast, our ME-STAD keeps a simple architecture design and has a good performance.

Different Strategies to Train Action Classification Action classification part is the other important part for ME-STAD. In this section, we will use different strategies to train and test our models to verify the effectiveness of our FCOS head. We vary the input of action classification head between training and testing, and verify the performance of our model.

The ablation results are in Table 3. From the table, we can find that:

- When testing with pre-extracted proposals, our model can have better performance than FCOS generated boxes. It is not surprising because we are performing actor localization with low-resolution inputs.
- However, our model still performs better than original proposal-based methods. Also, our model trained with sparse inputs (GT, Sparse FCOS outputs) performs worse than dense inputs with a more than 1% *mAP* gap. This result shows that we should use dense inputs to boost the classification

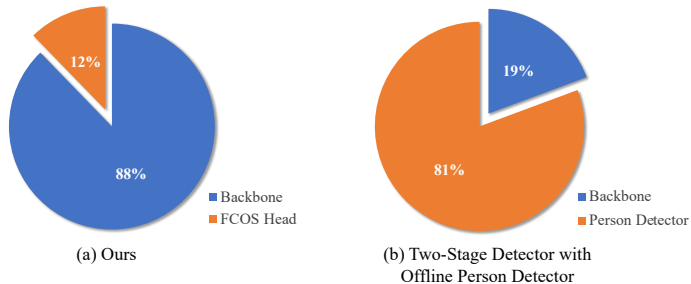


Figure 3. FLOPs pie chart with different parts in the spatial-temporal action detector. The left figure is our ME-STAD and the right figure is the proposal-based SlowFast. FLOPs of action classification head is ignored as the computation complexity of this part is too small. Both methods use the same SlowFast R50 backbone.

Method	λ_{cls}	λ_{unsup}	val mAP
ME-STAD	1	-	25.2
ME-STAD	10	-	25.5
ME-STAD	20	-	24.7
ME-STAD+TLA	10	0.2	26.8
ME-STAD+TLA	10	0.5	26.9
ME-STAD+TLA	10	1.0	26.5

Table 4. Ablation study on loss coefficients. We study the effect of different values for λ_{unsup} and λ_{cls} to verify the robustness of our ME-STAD.

Pseudo Label	Performance
None	25.5
EMA	26.0
Hard Threshold	26.0
Per Class Threshold	26.2
TLA	26.9

Table 5. Ablation study on different strategies to generate pseudo labels for the SSAD stage on AVA v2.2. We also report a strong baseline: training on annotated frames with EMA in the table.

performance. This can be an explanation of why WOO performs bad with Sparse-RCNN [36].

Ablations on Loss coefficients As stated in Sec. 3, we introduce λ_{cls} to balance the loss scale between actor localization and action classification task, and introduce λ_{unsup} to balance losses from labeled part and unlabeled part. Here, we make ablation experiments to show the robustness of each coefficient. Results in Table 3 support the robustness of different choices of λ_{cls} and λ_{unsup} . Model achieves the best performance when $\lambda_{cls} = 10$. Besides, when utilizing the unlabeled data, ablation experiments show that it’s better to set the ratio of loss weight between labeled part and unlabeled part to 2:1.

Computational Efficiency In this section, we will show the computational efficiency of our model under different input resolutions.

We vary the input resolution for our model during testing. The results are in Table 6. We can observe that with the default 256 input resolution, we perform

Models	Backbone	Input Res	Performance	FLOPs
SlowFast		256	24.7	97.5+406.5
WOO	R50, 8×8	320	25.4	147.5
Ours		256	25.5	111.3
Ours		320	26.1	173.8

Table 6. Ablation study on input resolutions on AVA v2.2. We use the square input, e.g., 256×256 to calculate the FLOPs for all our models. For WOO, we directly report the result from [5].

slightly better than WOO [5] and proposal-based SlowFast [7]. When we use a larger input resolution, i.e., 320, we can get a 0.6% performance boost and a slightly higher FLOPs than WOO [5] but much lower than proposal-based SlowFast.

Moreover, we analyse the component of different spatial-temporal action detectors, including proposal-based methods and our ME-STAD. The analysis results are in Fig. 3. From Fig. 3, we can easily observe that: FCOS head only occupies around 12% percent of the whole ME-STAD, and backbone action classification network has the majority computational complexity in ME-STAD. In contrast, the majority computational burden of two-stage detectors lies in the person detector part, which is redundant.

Ablations on Pseudo Label Generation For the semi-supervised action detection part, pseudo label generation is the critical part for this part. It’s a nature way to perform pseudo label generation by predicting the classification labels directly. However, as stated before, multi-label and long-tail classification problems make the SSAD part hard. In order to show the excellence of TLA, we explore different strategies to generate pseudo labels:

- **Hard Threshold.** We apply a hard threshold for all classes to filter generated pseudo boxes for all categories.
- **Per Class Threshold:** We apply independent threshold for each class in the dataset to filter generated pseudo boxes. The thresholds are calculated from the model on the training set.
- **TLA:** The method we proposed in Sec. 3.

For the former two strategies, we apply a temporal labeling restriction additionally to boost the performance: we remove classes which are not in the union set of surrounding annotated frames. Besides those semi-supervised techniques, we also try a strong but simple baseline: We discard the teacher model, and the model is learned with EMA on the annotated subset, then report the final result. The results are in Table 5.

From the table, we can see that: the commonly used hard threshold strategy does not work on the AVA dataset if we consider the influence of EMA. Even if we consider the multi-label and long-tail problems in the dataset, and have a stronger per class threshold baseline, it still have a minor performance gain over the baseline model. In contrast, our TLA along with SSAD has a better performance, which shows the effectiveness of TLA.

5 Conclusion

In this paper, we presented ME-STAD—an end-to-end method for spatial-temporal action detection. ME-STAD has a simple design and small computational burden, yet achieves significantly better results across the major spatial-temporal action detection dataset. The performance gain comes from two parts: one is the powerful anchor-free actor head. The other is the proposed novel semi-supervised training schema to utilize every piece of information in the training frame. We hope that our model, notwithstanding its simplicity, can en-light the broader problem of video understanding. We will continue to explore the multi-label and long-tailed problems existed in the spatial-temporal action detection.

A Appendix

This appendix provides further details of the main paper. We present extra experiments and visualizations. (1) Our ME-STAD can cooperate with stronger action classification heads; (2) The ablation of feature pyramid architecture; (3) Additional visualizations of TLA.

B Cooperating with stronger action classification heads

In this paper, we dive deep into building an end-to-end spatial-temporal action detector with minimum efforts. Contrary to [5,27] which highly rely on extra attention mechanisms, no additional attention module is introduced in our proposed ME-STAD. In order to show that our ME-STAD could also benefit from attention modules, we adopt a simple ACRN head [35] as the action classification head. Table 7 shows the experiment results. We could find that the basic ME-STAD could get 1.5% gains from the introduced simple ACRN head. Such results demonstrate that we could further boost the performance with other fancy attention modules, such as [35,28].

Method	Attention Module	val mAP
ME-STAD	None	25.5
ME-STAD	ACRN [35]	27.0

Table 7. Ablation study on classification head. We try to use ACRN [35] head as the classification head. Experiments are performed with SlowFast R50 backbone.

C Ablation of feature pyramid architecture

As shown in Fig. 2 in this paper, we build the feature pyramid (P3-P5) on top of features of keyframes from Res3 and Res4 layers. We adopt such an architecture after considering the balance of computation complexity and performance. We do extra experiments about adopting different feature pyramid architectures to perform actor localization. Experiment results are shown in Table 8. These results show that the architecture of the feature pyramid does not play the most essential role in ME-STAD. Although building P2-5 on Res2-4 could boost the performance from 25.5 to 26.0, it will introduce around 40% computation additionally. Hence, we select to build P3-P5 based on Res3 and Res4 to make a trade-off between the detector performance and computation complexity.

Method	Source	Target	val mAP	GFLOPs
ME-STAD	Res3-4	P3-5	25.5	111.3
ME-STAD	Res3-5	P3-5	25.2	113.4
ME-STAD	Res2-4	P2-5	26.0	152.8

Table 8. Ablation study on the architecture of feature pyramid. We try different feature pyramid architectures with SlowFast R50 backbone.

D Visualization of TLA

In Sec. 3, we propose a novel labeling strategy, i.e., the temporal label assignment (TLA), to better utilize every possible piece of information in sparse annotated spatial-temporal action detection datasets. TLA which utilizes the temporal restriction could provide more clear temporal action boundaries and fine-grained information to the detector. In Fig. 4, we visualize some results produced by TLA. The visualization results illustrate that TLA produces relatively reliable pseudo labels successfully on unlabeled frames. In addition, we find that there are often missing labels in provided ground-truth annotations which deteriorate the performance of the spatial-temporal action detector. Whereas, thanks to the promising actor localization ability of ME-STAD, TLA could detect most of the actors and assign dependable labels.



Figure 4. Visualization of results generated by TLA. Top row: the former neighbour keyframe with ground-truth annotations. Medium row: the later neighbour keyframe with ground-truth annotations. Bottom row: the frame labeled by TLA. Last column: a failure case. The figure is best viewed when zoomed in. Numbers of person proposals indicate the entity ids in keyframes with ground-truth annotations and assigned entity ids in frames labeled by TLA.

References

1. Arnab, A., Dehghani, M., Heigold, G., Sun, C., Lučić, M., Schmid, C.: ViViT: A video vision transformer. In: Int. Conf. Comput. Vis. pp. 6836–6846 (2021)

2. Berthelot, D., Carlini, N., Goodfellow, I., Papernot, N., Oliver, A., Raffel, C.A.: Mixmatch: A holistic approach to semi-supervised learning. *Adv. Neural Inform. Process. Syst.* **32** (2019)
3. Carion, N., Massa, F., Synnaeve, G., Usunier, N., Kirillov, A., Zagoruyko, S.: End-to-end object detection with transformers. In: *Eur. Conf. Comput. Vis.* pp. 213–229 (2020)
4. Carreira, J., Zisserman, A.: Quo vadis, action recognition? a new model and the kinetics dataset. In: *IEEE Conf. Comput. Vis. Pattern Recog.* pp. 6299–6308 (2017)
5. Chen, S., Sun, P., Xie, E., Ge, C., Wu, J., Ma, L., Shen, J., Luo, P.: Watch only once: An end-to-end video action detection framework. In: *Int. Conf. Comput. Vis.* pp. 8178–8187 (2021)
6. Fan, H., Xiong, B., Mangalam, K., Li, Y., Yan, Z., Malik, J., Feichtenhofer, C.: Multiscale vision transformers. In: *Int. Conf. Comput. Vis.* pp. 6824–6835 (2021)
7. Feichtenhofer, C., Fan, H., Malik, J., He, K.: SlowFast networks for video recognition. In: *Int. Conf. Comput. Vis.* pp. 6202–6211 (2019)
8. Girdhar, R., Carreira, J., Doersch, C., Zisserman, A.: A better baseline for AVA. *arXiv preprint arXiv:1807.10066* (2018)
9. Girdhar, R., Carreira, J., Doersch, C., Zisserman, A.: Video action transformer network. In: *IEEE Conf. Comput. Vis. Pattern Recog.* pp. 244–253 (2019)
10. Girshick, R.: Fast R-CNN. In: *Int. Conf. Comput. Vis.* pp. 1440–1448 (2015)
11. Girshick, R., Donahue, J., Darrell, T., Malik, J.: Rich feature hierarchies for accurate object detection and semantic segmentation. In: *IEEE Conf. Comput. Vis. Pattern Recog.* pp. 580–587 (2014)
12. Glorot, X., Bengio, Y.: Understanding the difficulty of training deep feedforward neural networks. In: *Int. Conf. Arti. Intell. Stat.* pp. 249–256 (2010)
13. Gu, C., Sun, C., Ross, D.A., Vondrick, C., Pantofaru, C., Li, Y., Vijayanarasimhan, S., Toderici, G., Ricco, S., Sukthankar, R., et al.: AVA: A video dataset of spatio-temporally localized atomic visual actions. In: *IEEE Conf. Comput. Vis. Pattern Recog.* pp. 6047–6056 (2018)
14. Jeong, J., Lee, S., Kim, J., Kwak, N.: Consistency-based semi-supervised learning for object detection. *Adv. Neural Inform. Process. Syst.* **32** (2019)
15. Köpüklü, O., Wei, X., Rigoll, G.: You only watch once: A unified CNN architecture for real-time spatiotemporal action localization. *arXiv preprint arXiv:1911.06644* (2019)
16. Kuhn, H.W.: The Hungarian method for the assignment problem. *Naval research logistics quarterly* **2**(1-2), 83–97 (1955)
17. Lee, D.H., et al.: Pseudo-label: The simple and efficient semi-supervised learning method for deep neural networks. In: *Int. Conf. Mach. Learn. Workshops.* p. 896 (2013)
18. Li, A., Thotakuri, M., Ross, D.A., Carreira, J., Vostrikov, A., Zisserman, A.: The AVA-Kinetics localized human actions video dataset. *arXiv preprint arXiv:2005.00214* (2020)
19. Li, D., Qiu, Z., Dai, Q., Yao, T., Mei, T.: Recurrent tubelet proposal and recognition networks for action detection. In: *ECCV.* pp. 303–318 (2018)
20. Li, X., Wang, W., Hu, X., Li, J., Tang, J., Yang, J.: Generalized focal loss v2: Learning reliable localization quality estimation for dense object detection. In: *IEEE Conf. Comput. Vis. Pattern Recog.* pp. 11632–11641 (2021)
21. Li, Y., Chen, L., He, R., Wang, Z., Wu, G., Wang, L.: MultiSports: A multi-person video dataset of spatio-temporally localized sports actions. In: *Int. Conf. Comput. Vis.* pp. 13536–13545 (2021)

22. Lin, T.Y., Goyal, P., Girshick, R., He, K., Dollár, P.: Focal loss for dense object detection. In: *Int. Conf. Comput. Vis.* pp. 2980–2988 (2017)
23. Lin, T.Y., Maire, M., Belongie, S., Hays, J., Perona, P., Ramanan, D., Dollár, P., Zitnick, C.L.: Microsoft COCO: Common objects in context. In: *Eur. Conf. Comput. Vis. LNCS*, vol. 8693, pp. 740–755 (2014)
24. Liu, W., Anguelov, D., Erhan, D., Szegedy, C., Reed, S., Fu, C.Y., Berg, A.C.: SSD: Single shot multibox detector. In: *Eur. Conf. Comput. Vis.* pp. 21–37 (2016)
25. Liu, Y.C., Ma, C.Y., He, Z., Kuo, C.W., Chen, K., Zhang, P., Wu, B., Kira, Z., Vajda, P.: Unbiased teacher for semi-supervised object detection. In: *Int. Conf. Learn. Represent.* pp. 1–13 (2021)
26. Liu, Z., Ning, J., Cao, Y., Wei, Y., Zhang, Z., Lin, S., Hu, H.: Video swin transformer. *arXiv preprint arXiv:2106.13230* (2021)
27. Mo, S., Xia, J., Tan, X., Raj, B.: Point3D: tracking actions as moving points with 3d cnns. In: *Brit. Mach. Vis. Conf.* pp. 1–14 (2021)
28. Pan, J., Chen, S., Shou, M.Z., Liu, Y., Shao, J., Li, H.: Actor-context-actor relation network for spatio-temporal action localization. In: *IEEE Conf. Comput. Vis. Pattern Recog.* pp. 464–474 (2021)
29. Paszke, A., Gross, S., Massa, F., Lerer, A., Bradbury, J., Chanan, G., Killeen, T., Lin, Z., Gimelshein, N., Antiga, L., et al.: PyTorch: An imperative style, high-performance deep learning library. In: *Adv. Neural Inform. Process. Syst.* vol. 32, pp. 1–12 (2019)
30. Rasmus, A., Berglund, M., Honkala, M., Valpola, H., Raiko, T.: Semi-supervised learning with ladder networks. *Adv. Neural Inform. Process. Syst.* **28** (2015)
31. Redmon, J., Divvala, S., Girshick, R., Farhadi, A.: You only look once: Unified, real-time object detection. In: *IEEE Conf. Comput. Vis. Pattern Recog.* pp. 779–788 (2016)
32. Ren, S., He, K., Girshick, R., Sun, J.: Faster R-CNN: Towards real-time object detection with region proposal networks. *Adv. Neural Inform. Process. Syst.* **28**, 1–9 (2015)
33. Rezatofghi, H., Tsoi, N., Gwak, J., Sadeghian, A., Reid, I., Savarese, S.: Generalized intersection over union: A metric and a loss for bounding box regression. In: *IEEE Conf. Comput. Vis. Pattern Recog.* pp. 658–666 (2019)
34. Sohn, K., Berthelot, D., Carlini, N., Zhang, Z., Zhang, H., Raffel, C.A., Cubuk, E.D., Kurakin, A., Li, C.L.: Fixmatch: Simplifying semi-supervised learning with consistency and confidence. *Adv. Neural Inform. Process. Syst.* **33**, 596–608 (2020)
35. Sun, C., Shrivastava, A., Vondrick, C., Murphy, K., Sukthankar, R., Schmid, C.: Actor-centric relation network. In: *ECCV*. pp. 318–334 (2018)
36. Sun, P., Zhang, R., Jiang, Y., Kong, T., Xu, C., Zhan, W., Tomizuka, M., Li, L., Yuan, Z., Wang, C., et al.: Sparse R-CNN: End-to-end object detection with learnable proposals. In: *IEEE Conf. Comput. Vis. Pattern Recog.* pp. 14454–14463 (2021)
37. Tarvainen, A., Valpola, H.: Mean teachers are better role models: Weight-averaged consistency targets improve semi-supervised deep learning results. *Adv. Neural Inform. Process. Syst.* **30** (2017)
38. Tian, Z., Shen, C., Chen, H., He, T.: FCOS: Fully convolutional one-stage object detection. In: *Int. Conf. Comput. Vis.* pp. 9627–9636 (2019)
39. Wang, G.H., Wu, J.: Repetitive reprediction deep decipher for semi-supervised learning. In: *AAAI*. pp. 6170–6177 (2020)
40. Wang, X., Girshick, R., Gupta, A., He, K.: Non-local neural networks. In: *Proceedings of the IEEE conference on computer vision and pattern recognition*. pp. 7794–7803 (2018)

41. Wu, C.Y., Feichtenhofer, C., Fan, H., He, K., Krahenbuhl, P., Girshick, R.: Long-term feature banks for detailed video understanding. In: IEEE Conf. Comput. Vis. Pattern Recog. pp. 284–293 (2019)
42. Wu, J., Kuang, Z., Wang, L., Zhang, W., Wu, G.: Context-aware RCNN: A baseline for action detection in videos. In: Eur. Conf. Comput. Vis. pp. 440–456 (2020)
43. Xie, Q., Dai, Z., Hovy, E., Luong, T., Le, Q.: Unsupervised data augmentation for consistency training. *Adv. Neural Inform. Process. Syst.* **33**, 6256–6268 (2020)
44. Xie, S., Girshick, R., Dollár, P., Tu, Z., He, K.: Aggregated residual transformations for deep neural networks. In: IEEE Conf. Comput. Vis. Pattern Recog. pp. 1492–1500 (2017)
45. Xu, M., Zhang, Z., Hu, H., Wang, J., Wang, L., Wei, F., Bai, X., Liu, Z.: End-to-end semi-supervised object detection with soft teacher. In: Int. Conf. Comput. Vis. pp. 3060–3069 (2021)
46. Yang, Q., Wei, X., Wang, B., Hua, X.S., Zhang, L.: Interactive self-training with mean teachers for semi-supervised object detection. In: IEEE Conf. Comput. Vis. Pattern Recog. pp. 5941–5950 (2021)
47. Zhang, Y., Tokmakov, P., Hebert, M., Schmid, C.: A structured model for action detection. In: IEEE Conf. Comput. Vis. Pattern Recog. pp. 9975–9984 (2019)
48. Zhou, X., Wang, D., Krähenbühl, P.: Objects as points. arXiv preprint arXiv:1904.07850 (2019)